Endmember detection in urban environments using hyperspectral HyMap data

K. Segl, U. Heiden, M. Müller and H. Kaufmann[a]

[a] GeoForschungsZentrum Postdam, Department 1 – Geodesy and Remote Sensing, Section 1.4 – Remote Sensing, Telegrafenberg, 14473 Potsdam, Germany, email: segl@gfz-potsdam.de

ABSTRACT

Many algorithms have been developed for supervised hyperspectral classification and spectral mixture analysis predominantly for geological and hydrological applications. Applications within the urban environments are still rare, although there exists a need for a time- and cost-efficient monitoring. Within the processing, the definition of representative spectral endmembers is the most time-consuming operation. In order to simplify this procedure, techniques such as Pixel Purity Index or matching techniques using spectral reference libraries were developed. However, urban surface materials possess spectral characteristics which prevent the use of standard processing tools. This is due to their high number combined with an extreme spectral variability caused by age, illumination and shadowing effects.

In this paper a spectral analysis tool is presented which automatically detects endmember spectra from the urban environment. It allows a faster processing of the hyperspectral images for urban applications in future. The tool consists of three major processing steps – spectral classification, post-processing and hyperspectral clustering. For the classification several Multi-Layer-Perceptrons (Artificial Neural Network) were used, which were trained by features derived from image spectra of three HyMap scenes. These scenes were necessary to make the tool more robust against effects resulting from atmospheric correction, image calibration, age of materials or illumination. Once the networks processed with a sufficient accuracy, the tool can be applied to any hyperspectral data set.

In this study the tool was used to derive endmember spectra from all HyMap scenes. The technique was capable to extract most representative spectral endmembers automatically minimizing the processing time significantly. However, it demands a good atmospheric correction and high spatial resolution of the sensor. Thus, the new approach enhances the exploitation of the information potential of the HyMap data for an area wide identification of urban surface cover types.

Keywords: Endmembers, neural networks, context information, spectral unmixing

1 INTRODUCTION

Advanced spectral analysis techniques, such as supervised classification or spectral unmixing, require the definition of spectral endmembers. This process is very time-consuming especially for hyperspectral data analyses. This is due to the greater variation of spectral surface characteristics recorded by the high spectral and spatial resolution of airborne sensors. In practice, there exist three methods for endmember detection - two image-based and one library-based approach. In the first method, a human operator examines the image and builds a spectral library of materials, which can be separated by their spectral characteristics. This is time-consuming but also very precise. The second technique is the Pixel Purity Index [1]. It is an unsupervised technique which extracts automatically the spectrally purest pixels. It repeatedly projects n-dimensional scatterplots onto a random unit vector and marks the extreme pixels located at the ends of the unit vector. However, this may not produce as many or as finely separated endmembers as desired by the user. This is especially true for urban analysis where a great variation of materials exists. Fig. 1 shows the spectral variation of PVC which is a commonly used roof material. All these spectra represent pure materials which will be predominantly not detected by the Pixel Purity Index. Additionally, the material type represented by the extracted spectra has to be determined by an operator.

Presented at the 3rd EARSeL Workshop on Imaging Spectroscopy, Herrsching, 13-16 May 2003

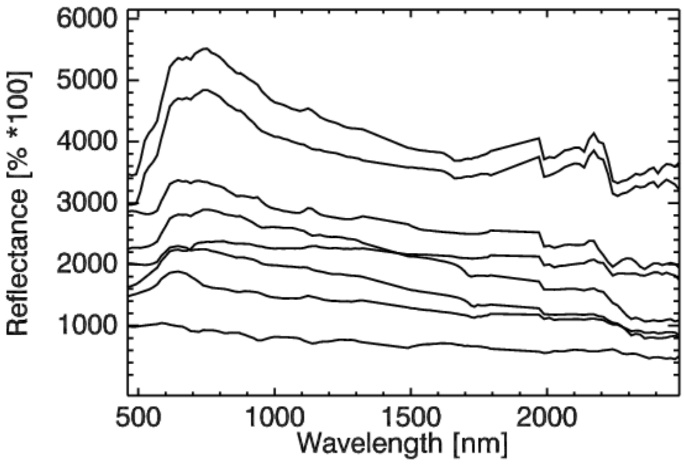

Figure 1. Spectral variations of PVC roofs caused by illumination and age.

The third approach uses a reference library including materials which are assumed to be in the image scene. However, there exist no standard library for urban surface cover types. The problem is that especially roof materials are highly variable due to age and pollution as well as illumination effects caused by the roof geometry, different solar zenith and azimut angles (Fig. 1). Thus, it seems to be impossible to store all variations which would be required for common use. Furthermore, laboratory measurements are not useful because such spectra may be significantly different from image spectra.

Based on these considerations the user-based approach has to be preferred. In this paper a spectral analysis tool is presented which simplifies this procedure. It automatically detects endmember spectra from the urban environment allowing a faster processing of the hyperspectral image data in future. The tool consists of three major processing steps – spectral classification, post-processing and hyperspectral clustering. Details about the applied techniques are described in the Approach (4). For the definition of the classification rules, features derived from three HyMap were necessary making the tool more robust against effects resulting from atmospheric correction, image calibration, age of materials or illumination.

2 TEST SITE AND IMAGE DATA

The test site for this investigation is a 2.7 km x 1.7 km north-south transect in the city of Dresden, Germany, showing a great variety of different urban structures and materials (Fig. 2). The HyMap data were recorded during a flight campaign carried out by the DLR (Deutsches Zentrum für Luft und Raumfahrt) with a pixel size of 3 m on August 1st, 2000, at 2 p.m. local summer time. The sensor has 126 bands from 437 to 2485 nm with bandwidths between 15 and 20 nm. An atmospheric correction was performed based on the ACORN software and a post-optimizing using the empirical line technique. For the geometric correction, a parametric approach was used incorporating a digital elevation model (DEM) of Dresden and information about the sensor’s position and orientation.

Additionally, two more HyMap scenes were included in this investigation. The first one covers the same area of Dresden and the second one the city of Potsdam, Germany. Both scenes were recorded with a pixel size of 6 m in May 1999.

3 DETERMINATION OF SURFACE COVER TYPES

Urban areas are characterized by a large variety of different surface cover types. Their successful automated identification requires a systematic analysis of the spectral characteristics of these surface materials. For this purpose, an inventory of urban surface materials was carried out first. 44 materials were identified and grouped into seven thematically and spectrally meaningful categories (Table 1). For all these materials, regions of interest (ROIs) were marked in the HyMap scenes. Altogether, nearly 17000 spectra were stored in a spectral library including material specific variations and data processing effects for further processing.

Table 1. Surface categories and materials used for endmember detection

roof materials	tiles (new), tiles (old), concrete, aluminum, zinc, copper, PVC, polyethylene, glass, plexiglass, bitumen bright/dark/red, tar-paper, schist, vegetation, gravel, facade, one still unknown material (other)
fully sealed materials	concrete, asphalt, tartan track, synthetics
partially sealed materials	cobblestone pavement, concrete, red /dark loose chipping trails
bare ground	sand, soil
water	river, pond, pool
vegetation	deciduous trees, coniferous trees, mixed forest, lawn, meadow, dry grass, field tilled, field untilled, fallow
shadow	falling on vegetation and non-vegetation

4 APPROACH

In this section, the three components of the new endmember detection tool are described represented by a spectral classification, a post-processing and a hyperspectral clustering. In the first step, significant features for material-oriented differentiation and a classification module are presented. In the second part, post-processing steps are described which select reliable objects from the classification result. Finally, spectral endmember variations are computed from the image scene using the spectra of the detected objects within a hyperspectral cluster analysis.

4.1 Spectral classification

4.1.1 Spectral characteristics

The spectral differentiation between the surface materials requires the definition and calculation of distinct spectral features. Since this process is difficult and time-consuming, an automatic feature detection program was used which lists the best features to separate two classes. Altogether, 45 computer-defined feature and 16 user-defined features were used after several optimization steps. The features can be grouped into four different types:

Depth of absorption bands. This feature represents a wavelength range where the electromagnetic radiation is highly absorbed by the surface material. The depth can be easily computed using the hull-function over the specific wavelength range. Typical materials that possess absorption maxima are e.g. aluminum, zinc and iron-based materials such as tiles or red-concrete. Thus, four different absorption bands of the VNIR wavelength range were used (840-960 nm , 844-860 nm , 984-1063 nm , 692-872 nm).

Ratios. A ratio enhances the spectral difference between two bands. It is simply calculated by the division of two bands. In this approach 51 ratios were selected for a better differentiation of all materials.

Mean. This feature represents the mean reflection of several adjacent bands. It allows the differentiation between darker and brighter materials. Four mean values were selected (430-460 nm, 430-2300 nm, 1500-1700 nm, 2100-2200 nm).

Root Mean Square Error (RMS) of a line regression. Materials such as PVC or sand show linear spectral reflection characteristics within a number of neighboring bands. This feature can be modeled by a line-regression leading to low RMS values for these materials. Two different wavelength ranges were used within this approach (646-1300 nm, 580-800 nm).

4.1.2 Classification module

In the next step, all 61 features were calculated for each spectrum of the library. These features serve as the input parameter of a classification model. Furthermore, they are used to define the classification rules for an automated detection of these materials. Various classification techniques were investigated to solve this task, selecting artificial neural networks as the most appropriate classifier. A multilayer perceptron (MLP) with one hidden layer was used for each class allowing a non-linear classification [2]. The number of input nodes varies between 16 and 22. The corresponding features and their number was defined during an iterative optimization of the class separability. The number of output nodes is 2 deciding between class and other-class. The supervised learning procedure was performed by a backpropagation algorithm with momentum. The number of hidden nodes and the learning rate were selected by a comparison of different network configurations.

After the 44 neural networks were adequately trained, the achieved differentiation of the library spectra was checked by the calculation of a confusion matrix. The overall accuracy was 90-100% for most materials. However, some materials could not be clearly separated. Problems remain for the dark categories shadow and water as well as for vegetation species due to their season-dependent characteristics.

Once the networks processed with a sufficient accuracy, the tool can be used for the spectral classification of the hyperspectra image data. Each neural network created a classification layer (mask) for its corresponding class.

4.2 Post-processing

Based on the classification result, the most accurate objects have to be determined and selected as endmembers. For this purpose, several post-processing steps were applied to the results. First, ambiguities in the class decisions were masked. Second, only objects with a minimum size of 20 pixels are regarded as significant and thus accurate. Smaller objects may probably include a higher fraction of mixed pixels. For the following analysis, vegetation, water and shadow classes were excluded since an automatic detection is not possible based on feature information of different image scenes.

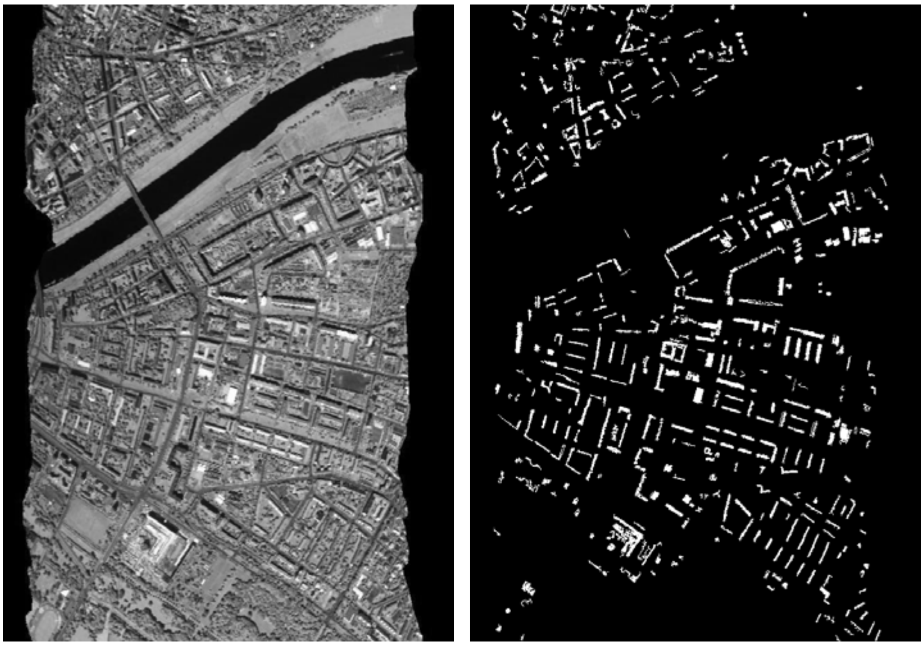

Figure 2. Grayscale subset of HyMap showing the test site in Dresden (left) and classified larger roof materials (right).

Most of the pixels representing roof materials can be used directly for the calculation of endmember spectra due to their high accurate identification (Fig. 2). However, roof materials such as bitumen and gravel show confusions with sealed classes since they consist of similar or identical materials. For the identification of reliable objects, information about areas of shadow was used which were classified by a MLP trained only with spectral features of the HyMap 2000 scene. Since buildings are connected with shadow only objects with a minimum distance and correct orientation towards a shadow segment were selected. This additional constraint reduces the number of detected objects. However, this is not so important since the darker materials possess only smaller spectral variations and thus a small number is sufficient.

Another special processing was applied to asphalt due to the confusion with roof materials such as dark bitumen and tar-paper. Based on the classification result only straight and long parts of objects were selected as reliable parts of streets.

4.3 Hyperspectral clustering

In the final processing step, the position of the detected materials is used to compute endmember spectra from the HyMap scene. For a better computation, these spectra have to be grouped into meaningful categories. Cluster algorithms can be used to identify important sub-categories in the multidimensional scatter plot of each material. In this approach, a cluster technique was used which minimizes the number of meaningful subclasses and optimizes gaussian distributions [3]. The algorithm uses a multivariate test to check the normality of the single subclusters but also to guide the algorithm in the high dimensional feature space for further cluster splittings. The maximum number of subclusters was set to 10.

5 RESULTS AND CONCLUSIONS

Within the test site, 35 different materials were detected and separated into 229 spectral endmembers. Fig. 3 shows some exemplary results of roofing concrete and red loose chipping trails. The spectra of both materials show the typical shape of the respective material characterized by iron-absorption and additional clay-absorption for the chipping trails. Besides, they also include a great variation in the albedos enabling a more precise comparison with image spectra in a final unmixing or classification procedure. Such spectral unmixing techniques which can deal with an extremly high number of urban endmembers are presented in [4] and [5].

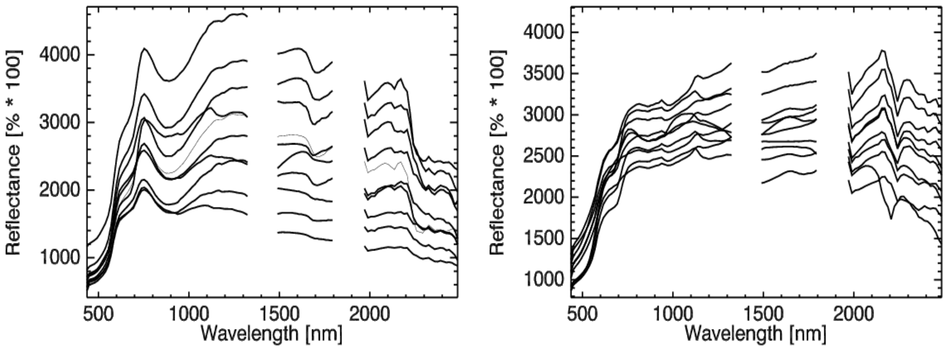

Figure 3. Detected spectral variations of roofing concrete (left) and red loose chipping trails (right).

In order to proof the transferability of the technique to other image data, additional endmembers from the scenes of Potsdam and Dresden (1999) were computed. Fig. 3 shows spectra of roofing concrete from Dresden and Potsdam in comparison.

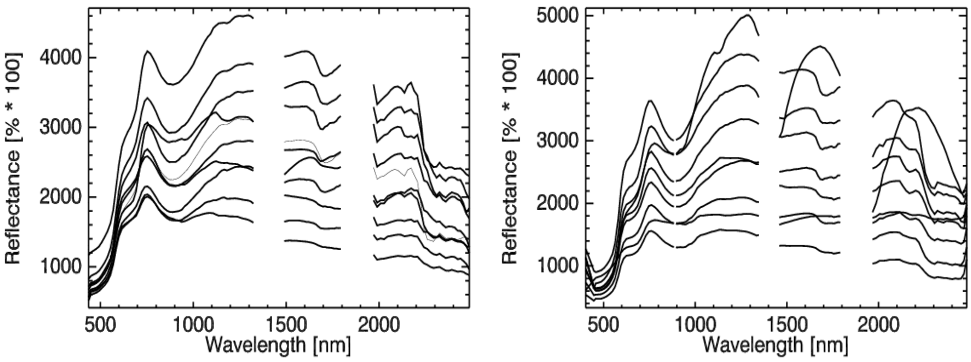

Figure 4. Spectral variations of roofing concrete in HyMap data of Dresden 2000 (left) and Potsdam 1999 (right).

Both spectra groups show similar features. However, there exist some variations in the Potsdam data and the overall shape of the spectra point to differences in the atmospheric correction. However, the algorithm was capable to deal with this problem. Thus, typical endmember spectra could be extracted for most roof, partially sealed and fully sealed materials. Only dark materials such as water and shadow cannot be identified in the images correctly, since their features depend in particular on the quality of the atmospheric correction. Similar problems arise for vegetation types because their features are season-dependent. Other dark materials such as roofing bitumen types and asphalt can only be clearly separated by additional shadow or straightness information. The incorporation of thermal bands will help to improve the spectral differentiation of all darker materials in the reflective wavelength range in future [5]. Besides higher emissivity values and their variations, differences in the surface temperature will help to separate roof materials from ground materials, because they are located at places characterized by different properties in regard to heating and cooling.

ACKNOWLEDGMENTS

This work was made possible by the flight campaign in 2000 carried out by the Deutsches Zentrum für Luft- und Raumfahrt Oberpfaffenhofen, Germany. The authors would also like to thank Integrated Spectronics Pty Ltd. for system correction and radiometric calibration of the HyMap Data.

REFERENCES

[1] BOARDMAN, J.W., KRUSE, F.A., and GREEN, R.O.: 1995, Mapping target signatures via partial unmixing of AVIRIS data: in summaries, Fifth JPL Airborn Earth Science Workshop, JPL Publication 95-1,v. 1, pp. 23-26.

[2] HORNIK, K., STINCHCOMBE, M., AND WHITE, H., 1989: Multilayer Feedforward Networks are Universial Approximators. Neural Networks, 2:pp. 359-366.

[3] SEGL, K., 1996: Integration von Form- und Spektralmerkmalen durch künstliche neuronale Netze bei der Satellitenbildklassifizierung.Deutsche Geodätische Kommission, Reihe C, Nr. 468,ISBN 3-7696-9508-9, München.

[4] ROESSNER, S., SEGL, K., HEIDEN, U., AND H. KAUFMANN, H., 2001: Automated differentiation of urban surface based on airborne hyperspectral imagery, *IEEE TGARS*, vol. 39, no. 7, pp. 1523–1532.

[5] SEGL, K., ROESSNER, S., HEIDEN, U., AND H. KAUFMANN, H., 2003: Fusion of spectral and shape features for identification of urban surface cover types using reflective and thermal hyperspectral data, *ISPRS Journal of Photogrammetry and Remote Sensing*, in press.